LASER APPLICATIONS AND OTHER TOPICS IN QUANTUM ELECTRONICS

# Drilling of sub-100 μm hourglass-shaped holes in diamond with femtosecond laser pulses

 

https://doi.org/10.1070/QEL17097

# Drilling of sub-100 μm hourglass-shaped holes in diamond with femtosecond laser pulses

B. Jeong, B. Lee, J.-H. Kim, J.-A. Choi, J. Yang, E.G. Sall, J.W. Kim, D. Heo, J. Jang, G.-H. Kim, V.E. Yashin

***Abstract.*** **We present images of microholes drilled in diamond using a homemade femtosecond Yb:KGW laser. We use a femtosecond laser source emitting pulses with a duration of 230 fs at a wavelength of 1030 nm, the focusing spot size amounting to 8.9 μm. The effect of the pulse energy and the number of pulses on the microhole geometry (hole diameter, circularity, taper angle, and drilling quality) is evaluated. The obtained results demonstrate the feasibility of drilling of hourglass-shaped holes in a diamond sample, which have similar diameters at the hole entrance (92 μm) and exit (95 μm), but a much smaller diameter (28 μm) at a certain waist section inside the hole.**

***Keywords:*** *femtosecond laser, ultrafast laser, laser micromachining, laser drilling, diamond.*

## 1. Introduction

Diamond is a distinctive material showing a variety of unique properties [1]. It is not only transparent in UV, visible and IR regions, but also has a high thermal conductivity greater than 20 W $cm^{-1}$ $K^{-1}$ at room temperature. Besides, it has unique radiation stability, chemical inertness, biocompatibility and a number of other important features, which determine numerous applications of this material. Microholes in diamonds with different diameters and taper angles at different hole depths have various applications. In particular, hourglass-shaped microholes whose diameters decrease and increase again after a certain depth can be applied to diamond dies for drawing.

Laser machining [2] is one important method to produce microholes and has several advantages such as high spatial resolution, no mechanical drilling-tool wear problem, good flexible shape, etc. Nanosecond lasers are traditionally used for drilling through holes. However, nanosecond pulses are too long when compared to the characteristic duration of laser radiation interaction with the materials. When nanosecond pulses are employed for drilling, the materials are heated relatively slowly, energy has much time to diffuse into the surrounding area before the affected spot is heated enough for the material removal, which produces a large heat affected zone (HAZ) [3].

Laser processing with femtosecond laser pulses can ionise a wide range of materials due to a high peak power and multiphoton absorption generated in the laser focus region and generate hot plasma at the interface while minimising HAZ [4]. Since the material is processed only in the vicinity of the focus point above the ablation threshold, it enables micromachining. High intensities within the focus volume result in multiphoton or tunnelling ionisation and subsequent avalanche ionisation. Substantial plasma generation and absorption enable the ablation of materials, such as transparent or low absorption materials, that are normally difficult to ablate by conventional lasers. This gives the unique capability of transparent material processing using a femtosecond laser [5, 6].

Diamond has been previously processed by a microsecond pulsed Nd:YAG laser and a nanosecond excimer laser [7]. Some aspects of diamond processing are described elsewhere [8–11]. To the best of the authors' knowledge, this paper is the first to study the method of drilling of hourglass-shaped holes with an unusually varying diameter in the hole depth in a diamond sample using a femtosecond laser.

## 2. Materials and methods

The schematic of a femtosecond laser-induced microdrilling system is shown in Fig. 1. The optical configuration of the system ensures the femtosecond laser beam delivery, optical imaging, and machining of the material. The system was extended based on a homemade femtosecond Yb:KGW chirped pulse amplification (CPA) laser [12, 13]. The laser has an average power of up to 10 W, a pulse duration of 230 fs, and a tunable pulse repetition rate from 50 kHz up to 500 kHz at a centre wavelength of 1030 nm. The output beam is a nearly symmetric Gaussian with $M^2 < 1.2$, and the maximum output pulse energy is 200 μJ. The pulse energy is controlled by the combination of a thin-film polariser and a half-wave

**B. Jeong** Electro-Medical Device Research Center, Korea Electrotechnology Research Institute, 111, Hanggaul-ro, Sangnok-gu, Ansan-si, Gyeonggi-do, Republic of Korea, 15588; Department of Creative IT Engineering, Pohang University of Science and Technology, 77 Cheongam-ro, Namgu, Pohang, Kyungbuk, Republic of Korea, 37673;
**B. Lee, J. Yang, E.G. Sall, J.W. Kim, D. Heo, G.-H. Kim** Electro-Medical Device Research Center, Korea Electrotechnology Research Institute, 111, Hanggaul-ro, Sangnok-gu, Ansan-si, Gyeonggi-do, Republic of Korea, 15588; e-mail: ghkim@keri.re.kr;
**J.-H. Kim, J.-A. Choi** GK UP, 64, Deokcheon-ro, Manan-gu, Anyang-si, Gyeonggi-do, Republic of Korea, 14087;
**J. Jang** Department of Creative IT Engineering, Pohang University of Science and Technology, 77 Cheongam-ro, Namgu, Pohang, Kyungbuk, Republic of Korea, 37673; School of Interdisciplinary Bioscience and Bioengineering, Pohang University of Science and Technology, 77 Cheongam-ro, Namgu, Pohang, Kyungbuk, Republic of Korea, 37673;
**V.E. Yashin** OJSC 'S.I. Vavilov State Optical Institute', Katetskaya liniya 5, korpus 2, 1999053 St. Petersburg, Russia

Received 18 July 2019; revision received 14 October 2019
*Kvantovaya Elektronika* **50** (2) 201–204 (2020)
Submitted in English

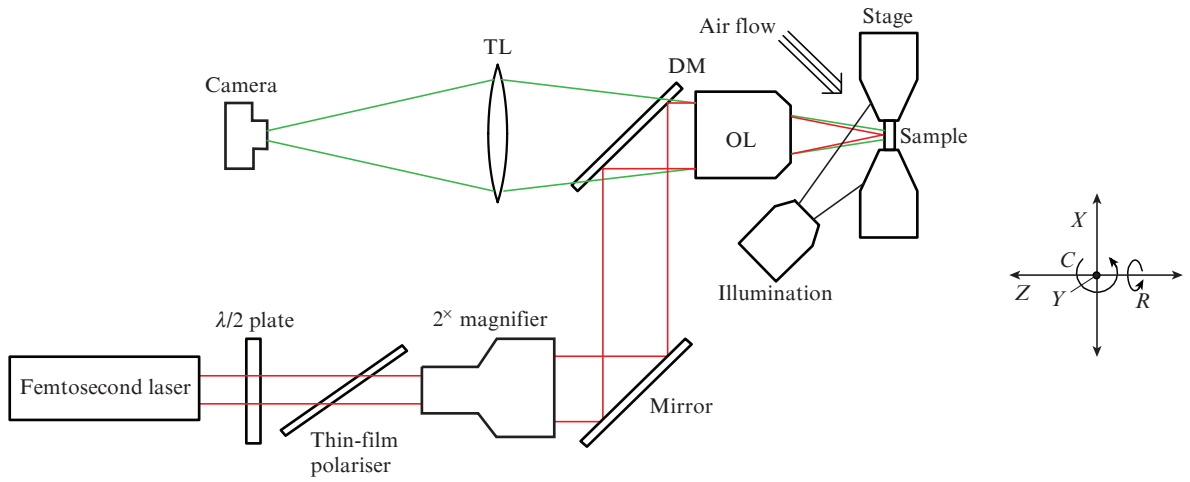


**Figure 1.** Schematic of the setup for microhole drilling: (TL) tube lens; (DM) dichroic mirror; (OL) objective lens.

plate mounted on a motorised rotation stage. The laser beam is magnified twice and reflected by a dichroic mirror and then it is focused at the sample by an objective lens (M Plan Apo NIR, 10×, NA = 0.26, Mitutoyo Co.). The size of the focal spot is about 8.9 μm.

The sample position was monitored with a computer controlled 5-axis translation stage: along three high precision linear translation axes ($X$, $Y$, $Z$) and around two rotation axes ($C$, $R$). The $X$ and $Y$ axes were perpendicular to the direction of laser pulse propagation in diamond and the $Z$ axis coincided with this direction. One of the rotation axes, $C$, was used for controlling the angle of the laser pulse incidence on the sample surface and for turning the front and rear of the sample surface. Another rotation axis ($R$) was used for sample processing upon its rotation at a speed of up to 1000 rpm. An electro-optic modulator in the CPA laser was used as a laser pulse shutter and was synchronised to the machining system.

After laser machining, the micro-topography of the drilled holes and cut features were characterised by an upright digital microscope. Then the detailed surface quality was measured and studied by a scanning electron microscopy (SEM). The basic materials used in this study were natural 360 μm to 420 μm thick diamonds mounted on the stainless steel holder supplied by the GK UP company.

## 3. Results and discussions

All experiments were performed at a pulse repetition rate of 500 kHz. First, we determined the focal plane position, where it coincided with the sample surface. The laser spot of the smallest machined area was designated as the focus position of the camera. Figure 2a shows the dependence of the ablation region diameter on the focal plane position (FPP) with respect to the sample surface. One can see that the ablation region diameter increases as the focal plane moves away from the sample surface. To determine the diamond ablation threshold, corresponding to the minimal energy required to initiate material removal, we measured the dependence of the size of the machining area on the laser fluence at the focus position on the sample surface (Fig. 2b) [14]. The extrapolation to zero of the linear fit yields the ablation threshold, which is 0.27 J cm$^{-2}$.

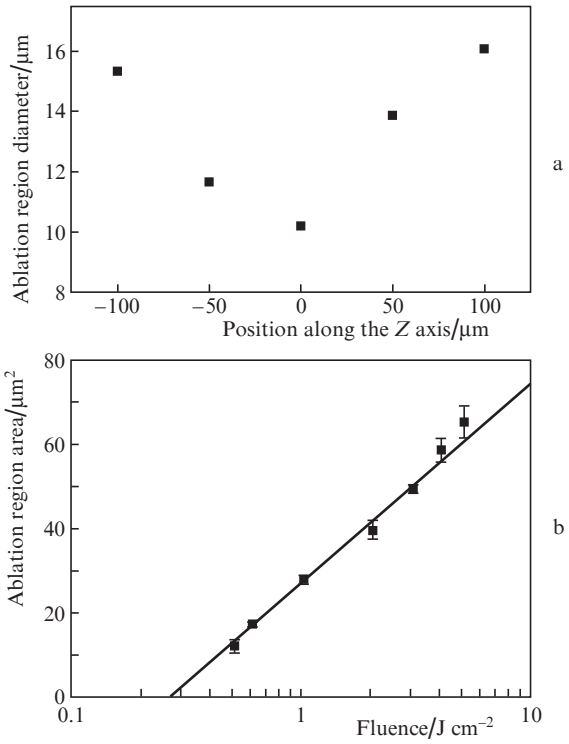


**Figure 2.** Dependences of (a) the ablation region diameter on FPP with respect to the sample and (b) ablated region area on fluence for diamond processed using a femtosecond laser.

Above or below the front surface, the FPP was considered as positive or negative, respectively (Fig. 3). The FPP was set positive to prevent the laser action on the inner layers of the material due to the low numerical aperture of the objective lens used in the experiment and to avoid the sample cracking caused by the laser heating.

Figures 4b and 4c show the SEM images of the drilled front and rear holes in diamond, respectively. Figure 4a shows the geometry of the hole. The laser output fluence was 3.1 J cm$^{-2}$. After cleaning the samples, the quality of the machined holes was evaluated. The taper angle $\theta$ of the holes in diamond was measured as follows:

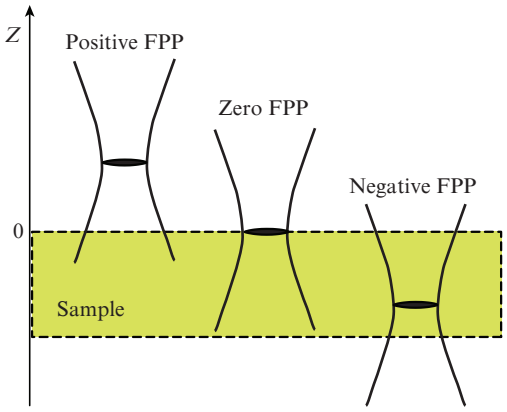


**Figure 3.** Schematic of focal plane positions on the sample.

$$\theta = 0.5\tan^{-1}\left(\frac{D_{ent} - D_{exit}}{2t}\right),$$

where $D_{ent}$ is the entrance hole diameter, $D_{exit}$ is the exit hole diameter, and $t$ is the thickness of the diamond sample. The holes had diameters $D_{ent}$ = 193 μm and $D_{exit}$ = 34 μm in a 420 μm thick diamond sample, which corresponds to $\theta$ = 20.7°. Figures 4b and 4c show the drilled holes that have good circular geometry for both entrance and exit sides and exhibit no microcracks or thermal damage. It can be observed that with the increase in laser power, the taper angle has been increased slightly along with the increment in both entrance and exit diameters of the fabricated microholes.

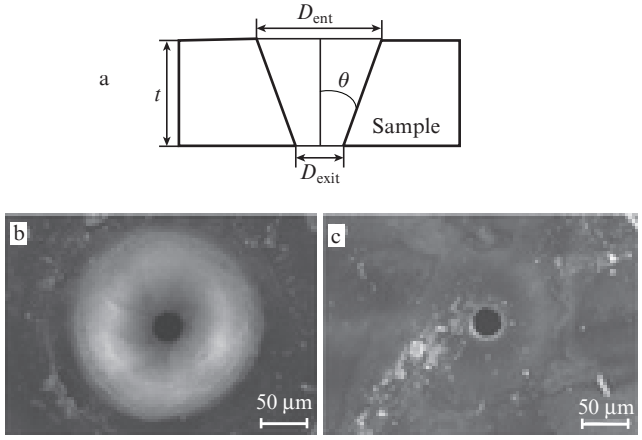


**Figure 4.** (a) Geometry of the hole and SEM images of (b) front and (c) rear holes.

Figure 5d shows the geometry of the hourglass-shaped hole. Figures 5a and 5b show SEM images of the drilled front and rear holes in diamond. Efforts were made to align the axes of the laser and the 5-axis stage to produce an hourglass-shaped hole. The front centre was aligned with the $X$, $Y$, $Z$ axes and with the rotation around the $R$ axis. After recording the $X$, $Y$, $Z$ coordinates, the sample was rotated around the $C$ axis to show the back surface of the diamond on the camera. Once again, the stage was used to find the back centre and coordinates were recorded. The front side of the hourglass

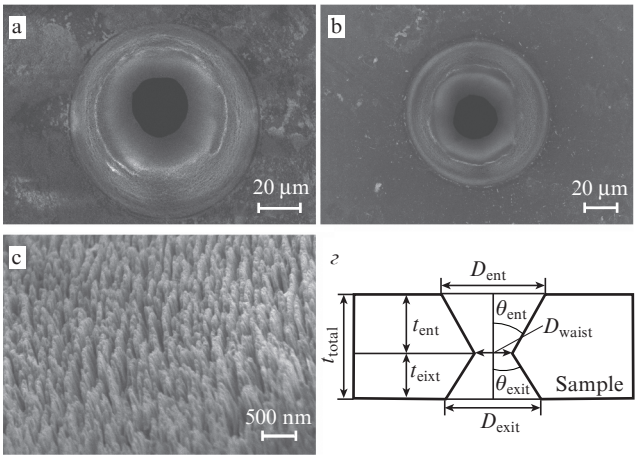


**Figure 5.** SEM images of the drilled (a) front and (b) rear holes in diamond as well as (c) entrance side of the hole and (d) geometry of the hourglass-shaped hole.

was processed sequentially, and the stage was rotated to the preset coordinates, and then the back side processing was performed. The laser fluence used here was equal to 2.1 J cm$^{-2}$.

In order to produce tapered holes on the front and back surfaces of the sample, the depth where the radius of processing was the smallest, was determined using a microscope. The diameters of the front and rear holes were 92 μm ($D_{ent}$) and 95 μm ($D_{exit}$), respectively. The diameter of the hole at the waist, $D_{waist}$, was 28 μm and the thickness of the used sample ($t_{total}$) was 420 μm, of which the depth from the entrance to the waist was $t_{ent}$ = 205 μm and the depth from the exit to the waist was $t_{exit}$ = 215 μm. Both the entrance and exit side taper angles ($\theta_{ent}$, $\theta_{exit}$) were measured as follows:

$$\theta_{ent(exit)} = 0.5\tan^{-1}\left(\frac{D_{ent(exit)} - D_{waist}}{2t}\right).$$

Both taper angles were equal to 16.7°.

Smooth surfaces are generally preferred for precision machining. Figure 5c shows the SEM image of the surface of the drilled hole in diamond. One can see a ripple for which the spacing is generally < 200 nm. The orientations of the ripple structures are parallel to each other. A similar ripple structure has been observed in various materials in the case of femtosecond laser drilling [15, 16].

It took four minutes to drill an hourglass-shaped hole in diamond. When machining holes of the same size, using femtosecond lasers generally takes longer to process than using nanosecond lasers, but clean and smooth holes are produced in this case. It is important to note that the actual turnaround time is shorter because it eliminates the need for post-processing in industrial applications. Also, when drilling with nanosecond and picosecond lasers, cracks are clearly visible around the exit side of the nanosecond laser perforations, and both the nanosecond and picosecond laser perforations show thermal damage [17]. The difference is mainly due to the fact that the femtosecond laser pulse duration is ultrashort compared to the timescale for thermal diffusion into the material. The accumulation of heat and mechanical stress on the material is greatly suppressed. The ability to drill such holes and hole arrays with consistent regular shape using femtosecond lasers is promising and remarkable due to the deterministic

nature of femtosecond laser–material interaction. Further improvement of the taper angle and aspect ratio can be achieved by using liquid-assisted rear side drilling [18, 19].

## 4. Conclusions

Femtosecond laser drilling is performed using a homemade Yb:KGW CPA system. Studies are presented on femtosecond laser drilling of small microholes with unusually varying diameters at different hole depths like an hour-glass shape hole. Drilling experiments are performed using natural diamond ablated with pulses having a duration of 230 fs, a pulse repetition rate of 500 kHz, and pulse energies from 1.25 μJ to 12.5 μJ at a wavelength of 1030 nm. Debris-free microholes with no thermal damage are produced in natural diamond. This laser drilling technique can be applied in the fabrication of microfluidic devices, photonic devices, sensors, and biomedical devices.

***Acknowledgements.*** This research was supported by the Primary Research Programme of the Korea Electrotechnology Research Institute (KERI) through the National Research Council of Science & Technology(NST) funded by the Ministry of Science and ICT (MSIT) (No. 16-12-N0101-85) and the MIST (Ministry of Science and ICT), Korea, under the ICT Consilience Creative Programme (IITP-2019-2011-1-00783) supervised by the IITP (Institute for Information & Communications Technology Planning & Evaluation).

## References

1. Komlenok M.S., Kononenko V.V., Ralchenko V.G., Pimenov S.M., Konov V.I. *Physics Procedia*, **12**, 37 (2011).
2. Tangwarodomnukun V., Mekloy S., Dumkum C., Prateepasen A. *J. Manuf. Processes*, **36**, 197 (2018).
3. Ihlemann J., Wolff B., Simon P. *Appl. Phys. A*, **54**, 363 (1992).
4. Venkatakrishnan K., Sudani N., Tan B. *J. Micromech. Microeng*., **18**, 075032 (2008).
5. Sugioka K., Cheng Y. *Light: Science & Application*, **3**, e149 (2014).
6. Gattass R.R., Mazur E. *Nat. Photonic*s, **2**, 219 (2008).
7. Windholz R., Molian P.A. *J. Mater. Sci*., **32**, 4295 (1997).
8. Kononenko T.V., Konov V.I., Garnov S.V., Danielius R., Piskarskas A., Tamoshauskas G., Dausinger F. *Quantum Electron*., **29**, 724 (1999) [*Kvantovaya Elektron*., **28**, 167 (1999)].
9. Kononenko V.V., Kononenko T.V., Pimenov S.M., Sinyavskii M.N., Konov V.I., Dausinger F. *Quantum Electron*., **35**, 252 (2005) [*Kvantovaya Elektron*., **35**, 252 (2005)].
10. Komlenok M.S., Kononenko V.V., Gololobov V.M., Konov V.I. *Quantum Electron*., **46**, 125 (2016) [*Kvantovaya Elektron*., **46**, 125 (2016)].
11. Kononenko V.V., Gololobov V.M., Pashinin V.P., Konov V.I. *Quantum Electron*., **46**, 899 (2016) [*Kvantovaya Elektron*., **46**, 899 (2016)].
12. Kim G.H., Yang J., Chizhov S.A., Sall E., Kulik A.V., Yashin V.E., Lee D.S., Kang U. *Opt. Express*, **20**, 3434 (2012).
13. Kim G.H., Yang J., Lee B., Sall E.G., Chizhov S.A., Yashin V.E., Kang U. *Quantum Electron*., **45**, 211 (2015) [*Kvantovaya Elektron*., **45**, 211 (2015)].
14. Choi W., Kim H.Y., Jeon J.W., Chang W.S., Cho S.-H. *Materials*, **10**, 212 (2017).
15. Tan B., Venkatakrishnan K. *J. Micromech. Microeng*., **16**, 1080 (2006).
16. Gräf S., Kunz C., Müller F.A. *Materials*, **10**, 933 (2017).
17. Momma C., Chichkov B.N., Nolte S., von Alvensleben F., Tünnermann A., Welling H., Wellegehausen B. *Opt. Commun*., **129**, 134 (1996).
18. Zhao X., Shin Y.C. *Appl. Phys. A*, **104**, 713 (2011).
19. Hwang D.J., Choi T.Y., Grigoropoulos C.P. *Appl. Phys. A*, **79**, 605 (2004).